ISSN 1064-2293, Eurasian Soil Science, 2021, Vol. 54, No. 10, pp. 1449–1462. © Pleiades Publishing, Ltd., 2021.
Russian Text © The Author(s), 2021, published in Pochvovedenie, 2021, No. 10, pp. 1167–1181.

GENESIS AND GEOGRAPHY OF SOILS

Early Pleistocene Pedosediments of the Lori Basin (Armenia): Genesis, Properties, and Paleogeographic Interpretation

A. V. Revunova[a, *], O. S. Khokhlova[b], and A. V. Rusakov[a]

[a] *St. Petersburg State University, St. Petersburg, 199034 Russia*

[b] *Institute of Physical, Chemical, and Biological Problems of Soil Science, Russian Academy of Sciences, Pushchino, 142290 Russia*

**e-mail: reina_abc@mail.ru*

Received December 23, 2020; revised April 30, 2021; accepted May 11, 2021

Abstract—Red-colored pedosediments were described in the sections of the Lori Basin in northern Armenia. The environmental conditions in the period of their formation have been reconstructed. The Early Pleistocene pedosediments in Yagdan and Kurtan-IV sections are available for study due to their conservation under the products of volcanic activity, which are dated earlier than 2 and 1.4 Ma, respectively. Prior to burial, the pedosediments were exposed to molten lava, which affected their composition and properties. We used the micromorphological method to study the pedosediments and determined the magnetic susceptibility, particle-size and total chemical composition, the content of carbon and nitrogen, and the biomorphs. Signs of the formation of the studied pedosediments in a humid warm (subtropical) climate were found, which corresponded to the results of earlier studies. Based on the combination of features, soil formations from the Yagdan section were assigned to Cambisols with Argic, Vitric, and Chromic qualifiers. Additional elements were input from the above layer of basalt lava to the sediments: copper, chromium, nickel, cobalt, and vanadium, which was reflected in an increase in the specific magnetic susceptibility and enabled us to specify the soil and sediments by geochemical coefficients. Pedosediments from Kurtan-IV section were characterized by Stagnic and Luvic features. They were also formed in a humid but cooler climate.

Keywords: paleosol, paleolandscape reconstruction, red-colored soils

DOI: 10.1134/S1064229321100100

INTRODUCTION

Red-colored soils are characterized by pronounced lithogenic features due to the presence of hematite in the soil-forming rock [25], which determines their specific color. They are formed in humid and semihumid tropics and subtropics under conditions of a deep percolative water regime [11, 16, 19]. Features of red-colored soil formation on the products of basalt weathering were discovered in the Lori Basin of Armenia during soil-archaeological expeditions in 2011–2019. Due to the quick burial under lava flows, the Early Pleistocene pedosediments were preserved and are available for study.

Paleosol studies of archaeological sites with hominid tools have been performed recently [27, 34, 38, 42, 50, 51]. They were accompanied by dating of the enclosing layers with or without evidences of soil formation on the basis of discovered archaeological artifacts and using various instrumental methods: direct (SIMS U–Pb, K–Ar, and $^{40}Ar/^{39}Ar$) and indirect (paleontological, magnetic, and micromorphological). As a result, the formation time of the studied red-colored soils was determined in the range of 2.5–1.4 Ma ago [50, 60].

Early Pleistocene paleosols are a very important and demanded geoarchive, the decoding of which is necessary for natural scientists to reconstruct the environmental conditions of the Early Pleistocene and to understand the history of landscape development and the paleoecological situation of the penetration of ancient humans deep into Eurasia. It has been revealed that air temperatures in the Early Pleistocene were higher than in the Middle and Late Pleistocene, which favored the migration of hominids to the north [34]. The climate in that period was subtropical, and the savanna-like vegetation was represented by hydrophilous meadows around water bodies and by xeromorphic grasses with single deciduous trees in automorphic positions (the data by A. Simakova according to [61]). The soils were assigned to Luvisols, Andosols, and Stagnic Cambisols [51]. In the Late Pleistocene, the climate became more moderate with meadow-forest vegetation, including coniferous plants (data by A. Simakova according to [61]). At the present time, the climate of the Lori Basin is continental-steppe of

the Asia Minor type [29]. Red-colored soils are not formed under such conditions.

In this work, we study not the classic red soils (Ferralsols, Nitisols, etc.), which are formed in tropical climate at mean annual temperatures above 28°C, but soils of higher latitudes, existing under conditions more close to those inherent to temperate climate. Weathering of mineral matrix and transformation of iron minerals in them are not as great as in the above-mentioned soils, so their red hue is not so intensive. The color is also affected by the parent rock: red hues are most pronounced in soils on limestone [39].

The aim of this work is to perform morphological-genetic diagnostics of buried Early Pleistocene red-colored pedosediments in the Lori Basin and reconstruction of paleoclimatic and paleolandscape conditions of their formation.

OBJECTS AND METHODS

The Lori Basin in the north of Armenia is an element of topography allocated to the synclinorium of the same name [39]. It is bordered by the Somkhet and Bazum folded ridges from the north and south and by the volcanic Javakheti Range from the west. The bottom and sides of the basin are composed of volcanic weakly alkaline basalts and basaltic andesites ~2 Ma old. They are covered by colluvial and lacustrine deposits. The modern relief and the river network were formed in the Quaternary period after the significant area uplift [60]. The mean altitude above sea level is 1700 m, and the topography is gently undulating. The climate is characterized by low temperatures (mean annual temperature is 10°C), and annual precipitation is 600–800 mm [4]. The mean monthly temperature varies from +15 to +20°C for the warmest month (July) and from 0 to +5°C for the coldest month (January) [2]. The plant cover is mainly formed by steppe vegetation, floodplain forests grow along river banks, and mountain forests are now cut down. Soils are mainly represented by mountain chernozems [2].

We have studied the outcrops discovered during reconnaissance surveys. Several sections made in them reveal the structure of Early Pleistocene soil-sedimentary strata. Similar formations were previously studied in the archaeological sections of the Lori Basin [51]. The absolute age of the studied deposits is determined by basalts and ash, which underlay and cover them.

We described two sections: Kurtan-IV (40°58′02.8″ N, 44°31′32.9″ E, h = 1309 m) and Yagdan (41°00′27.8″ N, 44°30′50.8″ E, h = 1277 m) named according to the nearest settlements (Fig. 1). The ash age in the central part of one of the quarry's walls (where the Kurtan-IV section is located) dated by the uranium-lead method (SIMS U–Pb) is 1.432 ± 0.028 Ma BP [55]. The age of the upper horizon of pumice sands is 1.495 ± 0.026 and 1.496 ± 0.021 Ma BP (according to SIMS U–Pb dating) [55], and 1.49 ± 0.01 Ma BP (by 39Ar/40Ar dating) (S. Hynek, personal message, cit. according to [5]). Fragments of fossil fauna were discovered during the quarry development: teeth of a rhinoceros assigned to the *Stephanorhinus hundsheimensis* species, which lived in the period of 1.4–0.5 Ma (M. Belmaker, oral report, cit. according to [5]). The sides of the canyons, on which section Yagdan is located, are covered by basalts and basalt andesites 2–2.5 million years old [60]. The pedosediments under them were formed prior to burial. The lava source is supposed to be at a distance of 45 km as the chain of volcanoes composing the Javakheti Range [61].

Mixed samples were taken from the layers of two studied sections to determine the magnetic susceptibility, particle-size and total composition and to perform CHN-analyses. The magnetic susceptibility and particle-size composition were determined in samples from section Yagdan taken from layers 1–5 and 7 (Fig. 2a) and in one sample from layer 3 of section Kurtan-IV. Monoliths for micromorphological study were taken from the center of each layer. We took one monolith from the center of layers 1, 2, 4, 5, and 7 in section Yagdan and one monolith from layer 3 in section Kurtan-IV. Samples for the bulk and CHN analyses were taken by one from the following layers: 1–5 and 7 in section Yagdan and 3 from section Kurtan-IV. Sampling from other layers was difficult due to abundant stones. Two samples—one from section Yagdan (layer 2) and one from section Kurtan-IV (layer 3)—were used for the analysis of phytoliths.

The specific magnetic susceptibility was determined on a Kappabridge KLY-2 Agico device (Czech Republic), and micromorphological analysis of the sections was performed under the AxioScopeA1 microscope, Carl Zeiss Microscopy GmbH (Germany), at the Center for Collective Use of the Institute of Physical, Chemical, and Biological Problems of Soil Science, Federal Research Center, Pushchino Scientific Center of Biological Researches, Russian Academy of Sciences. The bulk analysis was performed by the X-ray spectral fluorescence according to the methods of the Research Council for Analytical Methods of Research of the All-Russian Research Institute of Mineral Raw Materials on an AxiosMaxAdvanced, MalvernPanalytical sequential vacuum spectrometer (the Netherlands) at the Laboratory of Mineral Substance Analysis of the Institute of Geology of Ore Deposits, Russian Academy of Sciences. Glass-like disks were melted from weighted samples (they were preliminary ground to powder) by induction heating of a calcinated sample material with lithium borates at a temperature of 1200°C for the analysis of the main elements. The calcinated sample material was obtained after determining the losses during calcination at a temperature of 1000°C. Microelements were analyzed in preparations made by cold pressing of the dry sample substance with the addition of plastic filler.

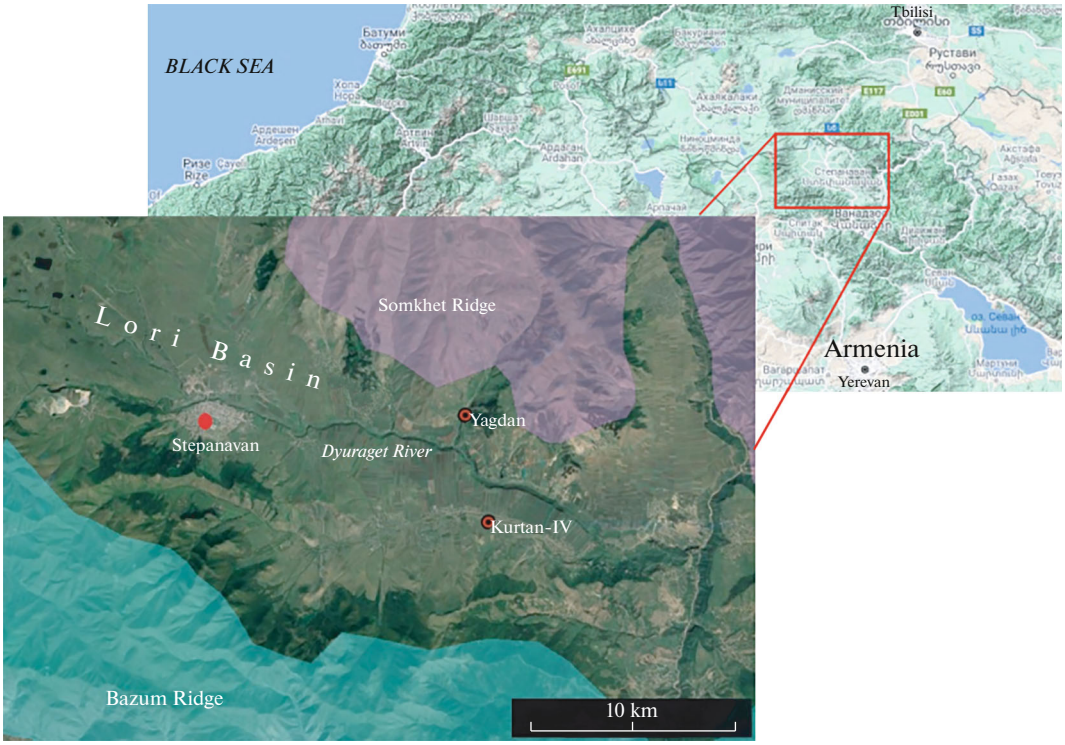

Fig. 1. The location of the studied sections in the Lori Basin, Armenia.

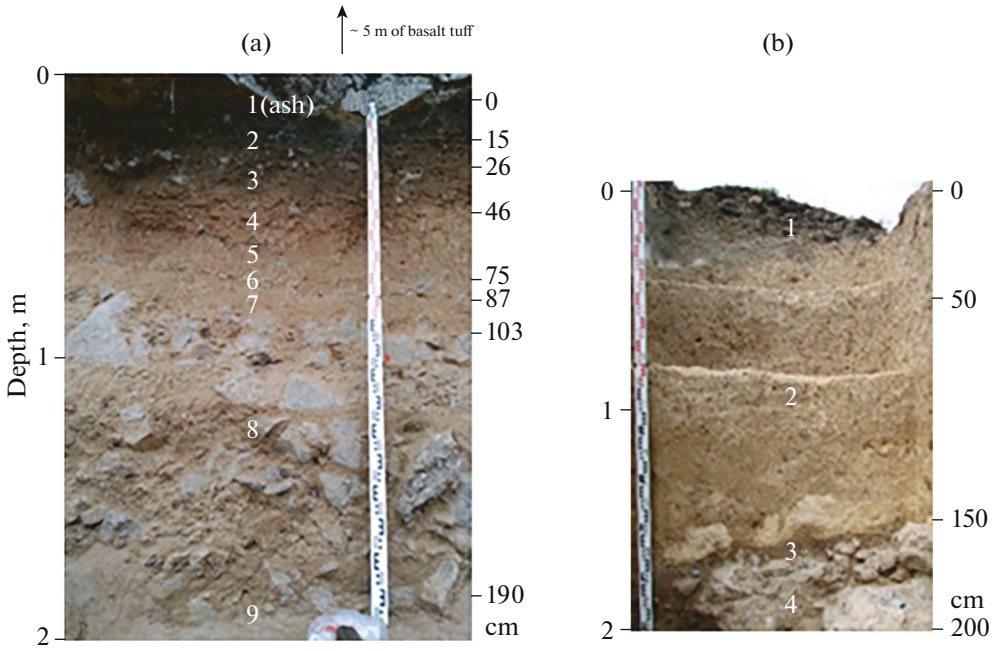

Fig. 2. Sections (a) Yagdan and (b) Kurtan-IV. Numbers in the center of the photographs are layer numbers.

The particle-size composition was determined by the pipette method, using sodium pyrophosphate for dispersion. The fractions were calculated per an absolutely dry weight taking into account the determined hygroscopic moisture [8].

A Leco CHN628 device (USA) was used for the CHN analysis. The study was performed at the Department of Soil Science and Soil Ecology of St. Petersburg State University. The operation principle of the analyzer was based on burning the samples in a resistance

furnace in a current of pure oxygen and then determining the content of gaseous carbon and hydrogen oxides by infrared spectroscopy and of nitrogen by the comparison of the thermal conductivity of gases.

The samples were macerated by conventional method [12] to isolate phytoliths. After boiling the sample in a 10% HCl solution to remove carbonates and organic matter, the sand and clay fractions were removed by the gravimetric method, and the residue was then separated in a centrifuge, using a heavy liquid. Phytoliths were extracted into the light fraction, which was placed on a filter, rinsed from heavy liquid, and dried. The samples were photographed, and all the revealed forms of phytoliths were counted, using a light microscope. The phytoliths were determined by freelance researcher of the Institute of Geography, Russian Academy of Sciences, Doc. Sci. (Geogr.) A.A. Gol'eva.

RESULTS OF THE RESEARCH

Morphological description. Section Yagdan was made in the left side of the canyon of the Mendzor Stream (a tributary of the Dzoraget River), on the southwestern slope of the Beyuktash Mountain. A layer of reddish-gray ground is exposed under a 5-m-thick layer of basalt. Eight layers visually identified in it are well pronounced along the whole outcrop (~17 m) (Fig. 2a).

The first layer 1-cm thick is represented by ash. The upper horizon of the soil that existed there was obviously burned due to high temperature of red-hot basalt lava flowing over the soil. The ash color is light ocherous with dark fine mottles. The material is dry, structureless, firm, hard, non-sticky, and non-plastic. There is no effervescence with 10% HCl. Neoformations are represented by iron streaks.

It is underlain by a series of four layers of total thickness of ~75 cm (layers 2–5) composed of dry loam with many inclusions of stones up to 15 cm in diameter. The layers are distinguished by color: black, brown, red, and ochreous colors are gradually alternating. Lighter mottles are visible on the background. The soil does not effervesce with 10% HCl.

Layer 6 at the depth from 75 to 87 cm is underlain by gravel. There are inclusions of stones of two types: dark compact with a light-colored weathering crust and light-colored granular. The color of the enclosing rock is ocherous. In the right part, the main layer is divided into two layers of smaller thickness, and gravel is coarser in the lower part of this series. There is a loamy interlayer, more light in color between the layers.

The underlying layer 7 (87–103 cm) is composed of light-colored ocherous loam with admixture of sand and with rare inclusions of fine gravel of two types (the light-colored one is fewer).

Layer 8 (103–190 cm) is formed by light-colored ocherous loam with admixture of sand and with abundant rock fragments and boulders 10–30 cm in diameter. They are mainly strongly weathered, light-colored gray, and granular. Small patches of loam without large stones contain few inclusions of gravel, 1–2 cm in size. This layer gives way to loam with few inclusions of stones 30–40 cm in diameter (layer 9, from the depth of 190 cm).

The Kurtan-IV section was studied in the north of the quarry, which is located on the left bank of the Dzoraget River, on the northeastern slope of the Surb-Sarkis Mountain. The modern soil (Fig. 2b, layer 1) from 30 to 60 cm thick (there is an erosion cut on its surface) is underlain by ash layer ~15 cm thick, which gives way to a layer of a mixture of sand and ash ~2 m thick (layer 2), covering the pedosediment (layer 3). It is formed on large basalt rounded blocks (layer 4). The color of the material in layer 3 is uniform light brown; the layer is weakly structured; and only abundant carbonate nodules (to 1 cm in diameter) effervesce with 10% HCl.

Since the color of the studied pedosediments is not intensively red, layer 3 of Kurtan section and layers 2–5 of Yagdan section of light brown color are assigned to red rocks of more moderate climate as compared to the humid tropical one.

Mesomorphology. Section Kurtan-IV, layer 3. Weakly cemented aggregated material. Large grains of silicates are visible, and there is fine earth between them. The color is reddish-pale yellow, and the content of manganese and iron is high. The material is porous, and the pores are lined by small agglomerated crystals of carbonates. Fragments of carbonate film with a cryptocrystalline structure are visible. There are evidences of textural differentiation in the main reddish-pale yellow mass: the presence of clay-iron films, subangular blocky structure, and the absence of introduced material (except for younger hydrogenic carbonates [51]).

Section Yagdan, layer 1. Silty, well aggregated material is characterized by spongy fabric. The accumulation of iron films and quartz grains is visible.

Layer 2. Slightly rounded weathered stone fragments covered by dusty material. There are abundant iron films, covering mineral grains.

Layer 4. Well-cemented material with visible isolated large grains of minerals. In general, the clay mass is more finely dispersed as compared to the upper layer. Iron is accumulated on grains of minerals, pores are visible, and the granular structure is pronounced.

Layer 5. The granular structure and iron accumulation are well seen, and manganic films not of volcanic origin are visible.

Layer 7. The material is well aggregated, iron accumulation and manganic films are formed.

Such properties as the presence of iron, clay, and manganic films, a pronounced granular structure, and

Table 1. Particle-size composition of layers in the sections studied.

Section and layer	Fractions (mm) content, %							
	1–0.25	0.25–0.05	0.05–0.01	0.01–0.005	0.005–0.001	<0.001	physical clay	physical sand
Yagdan								
layer 1	0.8	49.5	31.7	6.8	9.4	1.8	18.0	82.0
layer 2	1.1	41.5	32.8	8.8	4.0	12.0	24.7	75.3
layer 3	4.2	50.1	26.3	5.2	11.1	3.2	19.4	80.6
layer 4	0.1	31.5	33.5	12.3	17.8	4.8	34.9	65.1
layer 5	0.2	27.0	33.1	12.4	19.0	8.4	39.8	60.2
layer 7	0.1	30.5	23.9	9.9	22.5	13.0	45.4	54.6
Kurtan-IV	0.2	27.2	34.2	11.0	20.5	6.8	38.3	61.7

reddish and brown tints throughout the section may be identified as *cambic*.

Micromorphology. The mass of the sample from layer 3 of Kurtan-IV section is structured, iron neoformations of various forms are well pronounced: mottles (Fig. 3c), nodules, and detritus-like mottles (Fig. 3a). Mesofauna activity is visible (Fig. 3c). The iron-clay material is characterized by a clear fibrous, scaly, and cross-fibrous (Fig. 3a) and around-aggregate (Fig. 3c) orientation. Carbonate aggregates are visible in some microzones, they are composed of micrite and are covered by iron-clay material (Fig. 3b). Carbonates in Kurtan-IV section are hydrogenic: they were formed during the existence of a lake here in the Holocene [51].

No distinct structure in layer 1 (0–1 cm) of Yagdan section was recorded. Microzones with traces of strong waterlogging (iron and iron-manganic spots and streaks) (Fig. 3c) alternate with microzones, where the finely dispersed mass is characterized by a well seen optical orientation. This points to the development of displacement processes during the layer transformation (Fig. 3d). Iron is accumulated on the grains of primary minerals of volcanic origin (Fig. 3e).

A large content of iron and manganese is preserved in layer 2 (1–15 cm) of section Yagdan (Fig. 3f). Weathering of primary minerals is strong (Fig. 3g), as evidenced by the impossibility to see the minerals' shape in many cases and by iron or iron-manganic films on the surface of mineral grains, penetrating in them through cracks, and completely hiding the grains (Fig. 3h). This is a result of long-term intensive soil formation under climatic conditions, which were significantly warmer than now.

Evidences of soil formation in layer 4 (26–46 cm) are well pronounced: the structuring of fine earth (Fig. 3i), material reworking by mesofauna (Fig. 3j), and the orientation of iron-clay fine-dispersed substance around coarse solid particles (Fig. 3k) in combination with weak weathering of volcanic minerals, which may be explained by their input during new eruptions in the period of this layer formation.

Layer 5 (46–75 cm) is characterized by the preservation of strong iron accumulation in fine-dispersed material, iron-manganic or manganic mottles on its background, or films in pores (Fig. 3l). However, there are slightly weathered minerals (Fig. 3m), which testifies to a smaller temperature effect on soil during eruptions, which is also manifested in the change in color of the soil mass (Fig. 2a). There are few traces of mesofauna activity (Fig. 3n).

Iron accumulation in layer 7 (87–103 cm) is also pronounced; manganese is present as abundant iron-manganic films in pores (Fig. 3o); weathering of primary minerals is weak (Fig. 3p); and biogenic disintegration in pores is well seen (Fig. 3d).

Particle-size composition. Despite the fact that the particle-size composition is inherited from the initial parent rock, it is intensively transformed by soil processes during soil formation. Parent rocks in the studied area are represented by colluvium with stone fragments from the slope of Surb-Sarkis (Kurtan-IV), and alluvial and colluvial sediments of the Mendzor Stream and its tributaries (Yagdan) also with stony inclusions. Particles of physical sand—fine sand and coarse silt—predominate in Kurtan-IV section. However, 38% of physical clay enables its assignment to the medium loam. This separates it from enclosing sandy and sandy loam of colluvial provenance.

The amount of physical sand decreases and that of physical clay increases from top to bottom of Yagdan section. This regularity is violated by the presence of fractions of coarse and medium sand in layer 3. Percentage of physical clay increases at the expense of fine silt, and the clay content also increases in layers 2 and 7.

The CHN analysis. Organic carbon and nitrogen are important in soil-forming process [19], and the total carbon content in soil is on average 10–20 times greater than that of nitrogen [20]. Although carbonates, which are the main source of inorganic carbon, are absent in the studied pedosediments, an additional source may be its input as CO_2 in basalt lavas. We measured the content of nitrogen and total carbon to identify layers with the minimal C : N ratio, i.e. the layers,

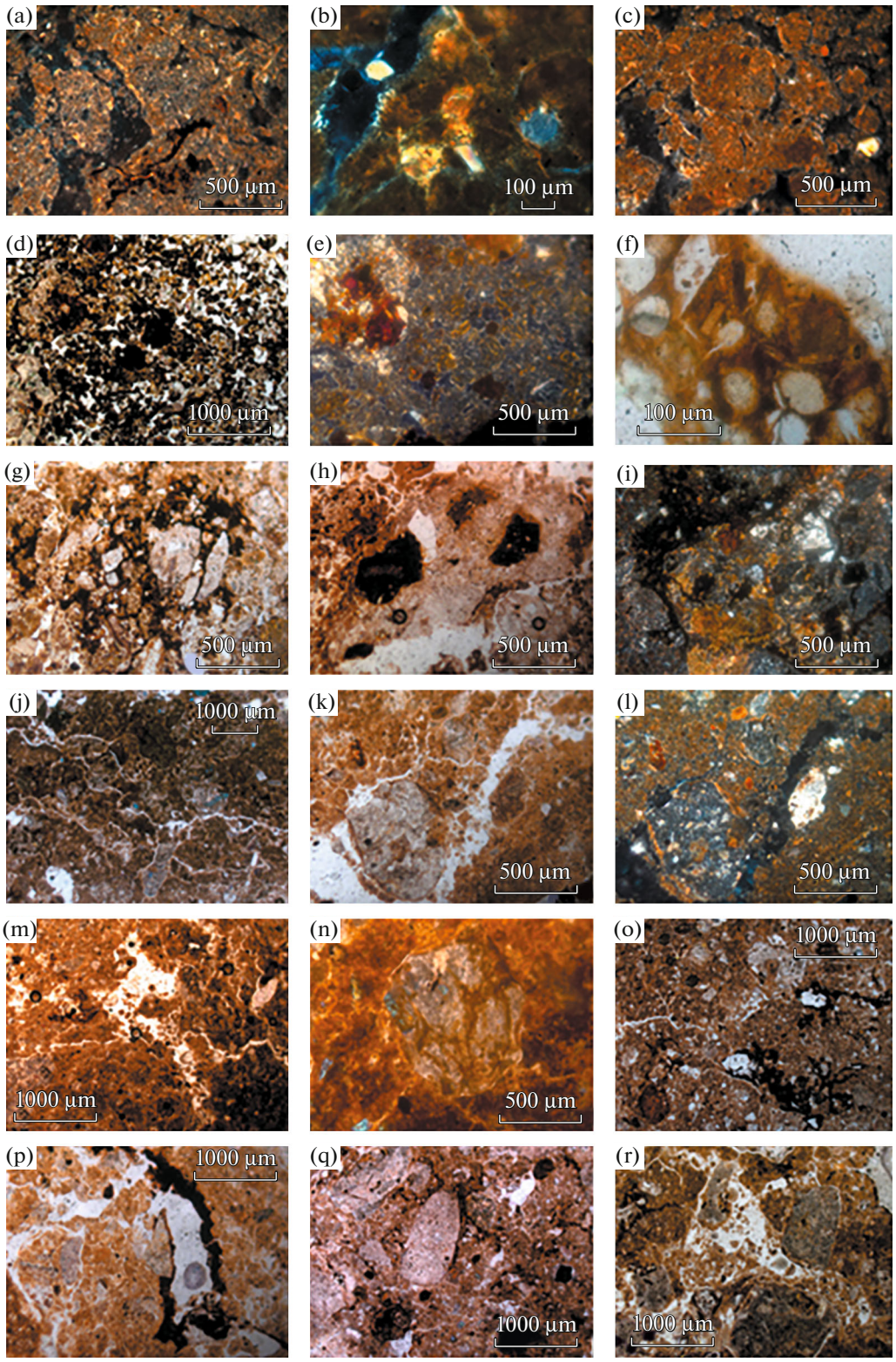

Fig. 3. Micromorphology of the studied pedosediments. **Kurtan-IV**: (a) iron neoformations: nodules, detritus-like mottles; fibrous, lamellar, and cross-fibrous orientation of iron-clay material; (b) grains of carbonates in the Fe-clay film; (c) iron concentrations, traces of mesofauna activity, orientation of the ferruginous-clay material around aggregates. **Yagdan, layer 1**: (d) general view; (e) lamellar, fibrous, or optical orientation of fine-dispersed material; (f) iron accumulation in fine-dispersed material around grains of the mineral skeleton; **layer 2:** (g) iron and iron–manganic films; (h) weathered volcanic minerals; (i) iron–manganic films; **layer 4:** (j) structured fine earth, (k, l) iron–clay substance, orientation around coarse soil particles; **layer 5:** (m) biogenic fragmentation, (n) weakly weathered mineral, (o) iron and manganic nodules; **layer 6:** (p) manganic cover of pore,(q) slightly weathered mineral, (r) biogenic fragmentation. The images were taken without analyzer (PPL) except for a, b, c, d, h, k, which were taken with the analyzer (XPL).

which were the most transformed by soil processes and in which the input of inorganic carbon as a result of volcanic processes was minimal.

The content of nitrogen in Kurtan-IV section is 0.05%, and that of carbon is 0.18%. The amount of these elements in the layers of Yagdan section is given in Table 2. Nitrogen and carbon content in this section does not exceed 0.07 and 0.45%, respectively, and noticeably decreases downward. The carbon and nitrogen content is maximal in layers 2 and 3.

Geochemical coefficients. Geochemical coefficients calculated on the basis of data of the total composition are used for quantitative characterization of changes in sediments due to soil formation and weathering. The following coefficients are the most indicative for the conditions of accumulation and transformation of the deposits studied (the coefficients are given in the text for Kurtan-IV section and in Fig. 4 for Yagdan section):

(1) The weathering coefficient (KW) $Al_2O_3/(CaO + Na_2O + K_2O + MgO)$ is the ratio of the content of aluminum oxide, which is the main clay component, to the content of oxides of soluble bases, entering the soil solution as a result of weathering of primary minerals [56, 57]. The KW is 2.20 for section Kurtan-IV. In Yagdan section, the KW of the upper horizon was affected by the lava flow, hence, is almost two times higher (4.22) than the KW of the underlying layers (2.26–2.55).

(2) The chemical weathering index (Rb/Sr) is based on the difference in the resistance of various minerals to weathering and is calculated as the ratio of Rb, which is associated with micas and potassium feldspar, to Sr associated with carbonates [48]. This index is 0.56 for Kurtan-IV section. In Yagdan section, the index sharply increases in the upper three layers from 0.26 to 0.67 and gradually rises to 0.85 in the lower layer.

(3) The coefficient $(Fe_2O_3 + MnO)/Al_2O_3$ shows the intensity of Fe and Mn oxidation in soil [36], which characterizes the oxidation rate of soil material in general [56, 57]. For Kurtan-IV section, the coefficient is 0.44. In Yagdan section, the pattern is similar to that of the KW.

(4) The carbonate enrichment index $(CaO + MgO)/Al_2O_3$ reflects the accumulation of soil calcite and dolomite [56, 57]. For Kurtan-IV section, the index is 0.31. In Yagdan section, it is very low, in the upper layer in particular, and varies from 0.14 to 0.20.

(5) Salinity index (sodium modulus) Na_2O/Al_2O_3 characterizes the behavior of easily soluble salts in the soil profile [56, 57]. Na_2O is a component of primary minerals in soil, mainly of sodium-containing feldspar. Its content may reach 5–6% in some elements of large fractions, but does not exceed 0.5–1% in the clay fraction [19]. The index is 0.040 for Kurtan-IV section. In Yagdan section, it is maximal in the third layer (0.069) and sharply decreases towards the upper horizon (0.025). In the lower three layers, the index varies slightly (0.046–0.049).

Table 2. Content of nitrogen and carbon in Yagdan section

Layer no.	Content, %	
	N	C
1	0.03	0.1
2	0.07	0.45
3	0.06	0.32
4	0.06	0.1
5	0.05	0.05
7	0.05	0.05

(6) The weathering parameter (titanium modulus) TiO_2/Al_2O_3 reflects the uniformity of material [7]. Aluminum and titanium are low-mobile elements because of low solubility of their oxides and hydroxides in cold water [46]. Consequently, the values of the Al/Ti ratio in residual soils may be considered close to those in the igneous parent rocks. Al is bound in them to clay minerals (kaolinite, illite, and smectite), micas, and feldspar. Ti is present in mafic minerals (olivine, pyroxene, hornblendite, biotite, chlorite, and ilmenite). These elements are slightly redistributed during the fluvial transportation of minerals, so their ratio is similar to that in the rocks of the weathering source [32]. Therefore, the TiO_2/Al_2O_3 ratio increases contrary to the SiO_2 content. The parameter is 0.060 for Kurtan-IV section. In Yagdan section, it decreases almost two times (from 0.076 to 0.039) from the upper to the third layer and gradually increases to 0.044 in lower layers.

Thus, the long-term development of the studied deposits is confirmed. It is revealed that after their formation, the pedosediments were strongly changed by physical and chemical processes due to the input of new material of different composition and properties. The changes are the strongest in the upper horizon of Yagdan section (its parameters in most cases differ sharply from lower layers) and are pronounced to layer 3 (including it) to a depth of 26 cm.

The distribution of trace elements in the studied sections is analyzed on the basis of data on the total composition.

The copper content varies widely: it is 203 and 199 ppm in the upper two horizons in Yagdan section and decreases from 68 to 30 in lower layers. In Kurtan section, the copper content is 48 ppm.

The zinc content gradually increases from the upper (203 ppm) to the lower (344 ppm) layer in Yagdan section. In Kurtan section, its content is low: 85 ppm.

The cobalt content in section Yagdan gradually decreases from 45 to 15 ppm. The regularity is different in layer 2: the cobalt content in it is less than in the

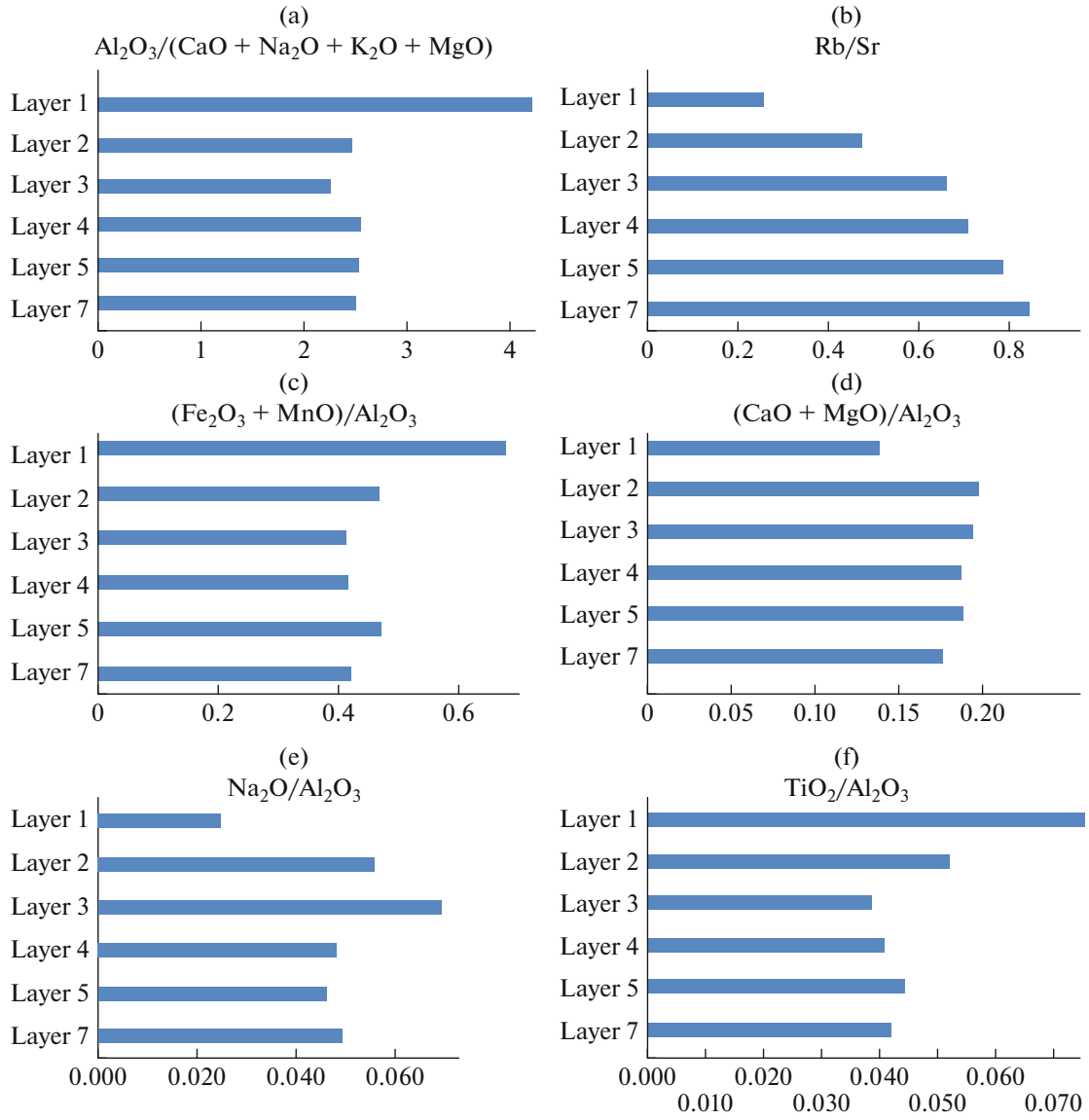

Fig. 4. Distribution of the coefficients of (a) weathering, (b) chemical weathering, (c) oxidation, (d) carbonate accumulation, (e) salinization, and (f) weathering of Ti and Al; Yagdan section.

underlying layer (18 and 22 ppm, respectively). In Kurtan section, the cobalt content is 20 ppm.

The lead content in the Yagdan section is irregular, but there is a noticeable trend for its rise downward (from 98 to 207 ppm). In Kurtan section, its content is much lower: 45 ppm.

The strontium content in the Yagdan section decreases downward from 244 to 181 ppm, starting from the second horizon. In the upper layer, its amount is 214 ppm. In Kurtan section, the content of strontium is lower: 199 ppm.

Chromium in Yagdan section is unevenly distributed: its content is the lowest in layer 3 (55 ppm) and is maximal in layer 2 (87 ppm). The second peak is detected in layer 5 (78 ppm). In Kurtan section, the content of chromium is relatively high and reaches 109 ppm.

The vanadium distribution pattern is also uneven. Its content increases towards layer 5 (136 ppm), but its maximum is detected in layer 1 of Yagdan section (147 ppm). In Kurtan section, it is slightly lower: 95 ppm.

Nickel content in Yagdan section is maximal in the upper horizon (143 ppm) and decreases to 37 ppm towards the third horizon. In Kurtan section, its content is 48 ppm.

Magnetic susceptibility (MS) is the total content of ferromagnetic substances or the total content of paramagnetic minerals and antiferromagnetic substances in case of small amounts of ferromagnetic material [3]. Measurement data on MS are often used in the study of soil-volcanic series, when eruption products stop soil development, to separate pure volcanic material and that affected by soil formation [59, 53]. Iron and

Table 3. Content of microelements in the studied sections, ppm

Section and layer	Cu	Zn	Co	Pb	Sr	Cr	V	Ni
Yagdan								
layer 1	203	203	45	98	214	82	147	143
layer 2	199	232	18	113	244	87	118	67
layer 3	68	245	22	156	243	55	122	37
layer 4	46	271	17	122	220	70	135	39
layer 5	42	324	16	223	193	78	136	43
layer 7	30	344	15	207	181	59	123	38
Kurtan-IV	48	85	20	45	199	109	95	63

its compounds determine a rise in MS in soil, because they are more widely spread as compared to other metals. Hematite, magnetite, and maghemite are the most common iron-containing minerals in the soil. They may be inherited from the parent rock or synthesized during soil formation. Manganese, nickel, and cobalt ions are strong magnetophoretic elements [3]. Magnetic minerals mainly enter the studied pedosediments from loose or consolidated covers erupted by volcanoes, surrounding the Lori Basin.

The specific MS of the studied samples widely varies between sections and down the profile. In Kurtan-IV section, MS is 63×10^{-8} m^3/kg. Data for various layers of Yagdan section are given in Fig. 5. The value is the highest in layer 1, i.e. in preserved ash of soil, which was in contact with basalt lava. It exceeds two times this parameter in the underlying layer 2 and 5–10 times the MS in not strongly transformed layers. In lower layers of Yagdan section, the MS gradually decreases, which is also similar to the distribution pattern of MS in the automorphic soil profile.

Phytoliths. Opal phytoliths are tiny particles of hydrated silicon dioxide dissolved in groundwater and absorbed by plant roots. They are transported by plant vascular system, become hard, and are accumulated in plant cells [54]. When plants die, phytoliths enter the soil with plant residues and are detected in fine earth in fractions less than 0.1 mm as silica bodies of relatively regular shapes. These particles enable the identification of plants after a long time period [12].

Phytoliths were found in layer 2 of Yagdan section and in Kurtan-IV section. Phytoliths in the samples from Yagdan section are typical for the modern vegetation of grass meadow-steppes [29] and obviously do not represent plants of the period, when this layer was formed. They are rather the remains of modern plants brought into this layer. The sample from Kurtan-IV section contains phytoliths of wormwood, coniferous, and lacustrine plants (Table 4), which do not occur in the studied area at the present time and cannot coexist. This combination indicates that the studied sample is a pedosediment, which underwent significant diagenetic processing after the end of functioning and burial. It includes the following groups of plants designated by numbers: 1—dicotyledonous herbs; 2—coniferous; 3—forest grasses; 4—meadow grasses; 5—steppe grasses; 6—arid grasses; 7—wormwood; 8—*Phragmites/Scirpus*; and 9—plant fragments and incompletely formed unidentified groups.

DISCUSSION

The pedosediment from Kurtan- section is covered by a mixture of sand and ash, the age of which is dated

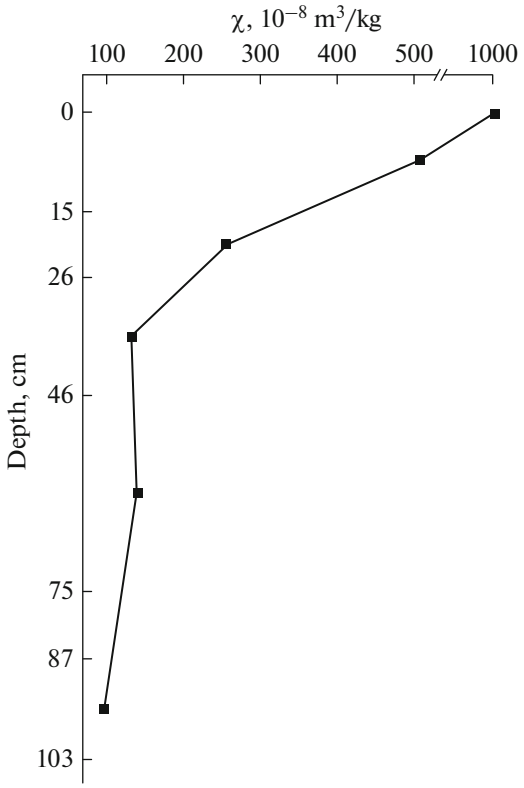

Fig. 5. Variability of the magnetic susceptibility index in the Yagdan section.

Table 4. Content of some groups of phytoliths, %

Sample	Phytoliths, number/%	1	2	3	4	5	6	7	8	9
Yagdan, layer 2	8/100	75	–	–	25	–	–	–	–	–
Kurtan-IV	130/100	23	14	–	16	11	2	18	2	14

about 1.4 Ma [55]. The blocky subangular structure, the increased content of biogenic elements (strontium), and the pronounced mobility and orientation of iron-clay material detected by meso- and microobservations indicate that the sediments were transformed by soil-forming processes. The orientation of iron-clay material enables us to suggest that there is an illuvial component in the preserved horizon of the studied pedosediment, i.e. the evidence of Luvisols. The texture of the pedosediment is medium-loamy [18], which distinguishes it from the surrounding sandy and sandy loamy deluvial deposits.

The nitrogen content in the studied layer of Kurtan-IV section is 0.05%, and the carbon content is 0.18%. The ratio between the elements is wide: nitrogen comprises 36% of carbon (contrary to 10–20% for recent soils [20]). This phenomenon occurs in paleosols [41, 58] and probably indicates an intensive mineralization of nitrogen under optimal humidity and sufficient amount of nitrogen-rich organic matter in the period of soil formation. After the soil was covered by lacustrine sediments, oxygen inflow into it stopped, and nitrogen was deposited (not mineralized) [41]. It should be pointed out that paleosols of the age below 10000 years were studied in the above referenced works.

The weathering coefficient (2.20 or 79%) and the titanium modulus (0.06) reflect a significant weathering of the initial material, which could be a result of long-term soil formation in humid climate. However, this index does not reach the values typical for the upper horizons of tropical soils formed on volcanic rocks, for example, in Vietnam (the KW in samples of postlithogenic uneroded soils exceeds 95%) [42] and Cameroon (the KW of all soil samples exceeds 95%) [52].

We assume that owing to the location of Kurtan-IV section at high altitude, soils were not covered by lavas, and the period of their formation was longer as compared to soils of Yagdan. This is confirmed by a small content of volcanogenic elements (copper, zinc, cobalt, and nickel) and low MS (Fineatal 1989, cited in [14]). According to the reconstruction, the area was flooded by a lake in the Holocene [51], which could also cause a decrease in the specific MS. After that, it was covered by colluvial sand and pebble deposits, as a result of which, the SiO_2 content in the layer increased contrary to that of such strong magnetophoretic elements as manganese, nickel, and cobalt compounds [3]. The index of carbonate enrichment is relatively high, which corresponds to the presence of diagenetic lacustrine carbonates.

The revealed phytolith complex is a mixture of adventive and indigenous plants: coniferous and wormwood, meadow and arid grasses, and *Phragmites/Scirpus*. The presence of coniferous is of particular interest, because they do not grow near the section now. According to the palynological analysis performed by A. Simakova for the Early and Middle Pleistocene sections of the Lori Basin [60], red-colored soils were formed in the Early Pleistocene, when the plains were dominated by savanna-like vegetation with a large portion of meadow herbs, and mountain slopes were covered by coniferous–broad-leaved forests.

Taking into account the presence of detritus-like mottles and iron nodules (Figs. 3a, 3c), it may be assumed that there were periods of moisture stagnation in the upper (which is absent now) horizon, therefore, the qualifier *stagnic* is used to determine the classification position of the pedosediment without the upper layer.

Pedosediments of Yagdan section also bear signs of formation in past climatic epochs. They are more than 2–2.5 million years old (according to the covering sediments). The soil structure is pronounced, and mineral grains are covered by clay-iron films.

Clay minerals revealed in thin sections from samples of the upper horizons may be a result of pelitization under the effect of postmagmatic solutions [24], and the red color is related to the adsorption of iron oxides. Their appearance is a consequence of humid tropical or subtropical climate. Iron films revealed in thin sections of layer 3 completely cover the grains of volcanic minerals and are a result of long-term and intensive processes of soil formation under significantly warmer and wetter climatic conditions than the modern ones. Layer 4 bears pronounced evidences of soil formation: structured mass, castings of mesofauna, and orientation of iron-clay fine-dispersed material around coarse soil particles. There are traces of vital activity of soil fauna in layer 5. The percentage of large particle-size fractions in Yagdan section decreases with depth. The particle-size composition changes from coarse-silt light loam to silt heavy loam, which may also testify to a longer formation period of re-deposited sedimentary rocks, on which soils of Yagdan are formed. The carbon content sharply rises in layers 2 and 3, which corresponds to an increased content of nitrogen, whose origin may be only biogenic. Thus, the features of Cambisols are clearly seen in the section: clay, iron, and manganic films, the particle-size composition not lighter than light loam, and brown and reddish hues.

The maximal weathering coefficient is recorded in the upper layer of Yagdan section (Fig. 4a), which was affected by hot flowing lava. In the lower layers of the section, the coefficient is evenly distributed and is ~2.5, which indicates strong weathering. The coefficient of chemical weathering in the upper horizon of Yagdan section (Fig. 4b) is minimal and increases downward, which confirms the strong temperature effect on the soil profile from above. The oxidation coefficient in the upper layer of Yagdan section is maximal (Fig. 4c) and differs of the coefficients of the underlying layers, which points to specific development features of the upper layer. In general, the coefficient varies slightly downward, indicating the absence of an oxidative barrier in it. A very low salinity index confirms the formation in the humid climate. A relatively high titanium modulus is recorded in the upper layers of Yagdan section (Fig. 4f). We assume that this is a result of the input of additional material by volcanic processes after soil formation.

The upper two layers in Yagdan section are pronouncedly distinguished by the content of copper, cobalt, nickel, chromium, and vanadium. These elements are not accumulated in living organisms [26], but are abundant in basalt lavas [22]. Zinc is strictly related to the humus horizon. This is explained by its high biological significance and a tendency to biogenic accumulation [26]. There is also a lot of zinc in basalts [22]. The element is actively transferred by plants from the humus horizon to the underlying layer [26]. The highest zinc content in Yagdan section is found in the lowest horizon, which may indicate a long-term soil formation. Strontium is the only microelement in Yagdan section with pronounced maximums in layers 2 and 3. This is probably explained by its ability to be accumulated in plants [21].

An increase in the amount of iron, chromium, nickel, zinc, vanadium, and lead, which are strongly related to mafic igneous rocks [22], is also seen in layer 5 of Yagdan section. Taking into account a slight increase in the MS index in this layer, it may be assumed that there are traces of volcanic emissions (well transformed by soil-forming processes) or of the input of material from the slope. The horizon may correspond to the *vitric* qualifier.

Layers 2 and 7 are distinguished by the amount of clay particles (12 and 13%, respectively) and can be attributed to argic horizons. The high content of clay particles is suplemented by clay films in the overlying horizons and the optical orientation of the finely dispersed mass.

A sharp increase in the MS of layer 1 of section Yagdan reflects the strong impact of the lava flow. Below the layer 3, the MS is low and evenly distributed.

Ancient phytoliths are not found in the section, which may be related to the fact that these are soils without the upper horizons affected by hot lava.

CONCLUSIONS

It is confirmed that the pedosediments revealed in the Lori Basin were formed under climatic conditions that differed from the modern ones. Climate changes during soil formation are reconstructed. The studied sediments are transformed by soil-forming processes, which is indicated by the structured soil mass; castings of mesofauna; biogenic fragmentation; the orientation of iron-clay material around coarse soil particles; and the increased content of nitrogen, carbon, strontium, and zinc in layers 2 and 3 of Yagdan section.

The pedosediments are approximately dated by the overlying and underlying sediments, as well as by tools found in them (Early Acheul in Yagdan section [6] and Early-Middle Acheul in Kurtan-IV section [5]). The age is 2–2.5 Ma for Yagdan section and 1.4 Ma for Kurtan section. Pedosediments from Yagdan section were covered by lava in the period with humid climate. This is confirmed by the presence of manganic-iron and clay films, low carbonate content and salinity indexes, along a relatively high weathering index. According to the reconstruction [60], the relief of the Lori Basin more than 2 Ma ago was in general low-mountainous, and phytoliths of savanna-like vegetation found in the horizons of the same age dated by the Early Pleistocene testified to subtropical conditions. The climate in the period of the formation of pedosediments in Yagdan section could be subtropical, because the weathering coefficients in them did not reach the values typical for red-colored soils on volcanic deposits formed in the modern tropical climate. Pedosediments from Yagdan section may be assigned to *Cambisols* with *Vitric, argic(?),* and *Chromic* qualifiers (brown forest illuvial reddish soils with volcanogenic inclusions).

Pedosediments in Kurtan-IV section were also formed under humid but cooler climatic conditions. They are distinguished by illuviation traces in the form of pronounced optical orientation of clay material and by water stagnation as seen from the development of various iron neoformations. The area was uplifted simultaneously with the Caspian Sea regression [59], which resulted in the appearance of coniferous plants, which phytoliths were found during the previous studies [59] and in samples taken in 2018. Pedosediments from Kurtan-IV section may be assigned to Stagnic Luvisols (surface-gley or gley).

Factors, which affected the preservation of pedosediments and changes in their composition and properties in later periods, were identified and confirmed. The upper horizon of Yagdan section strongly differs from the underlying ones by increased weathering and oxidation, and these properties were also found in layer 3. It is characterized by increased MS, as well as of the content of copper, cobalt, nickel, vanadium, and chromium input from basalt lava.

ACKNOWLEDGMENTS

The authors are grateful to E.V. Belyaeva for the opportunity to participate in terrain work, to Senior lecturer of the Department of Physical Geography and Landscape Planning of St. Petersburg State University A.G. Ryumin for the performing CHN analysis, and to freelance researcher of the Department of Soil Geography and Evolution of the Institute of Geography, Russian Academy of Sciences, Doc. Sci. (Geogr.) A.A. Gol'eva for the analysis of phytoliths.

FUNDING

This work was supported by the Russian Foundation for Basic Research, projects nos. 18-00-00592 and 19-29-05024-mk. The micromorphological analysis was performed on the equipment of the Common Use Center of the Institute of Physical, Chemical, and Biological Problems of Soil Science, Russian Academy of Sciences within the framework of state assignment no. 0191-2019-0046.

CONFLICT OF INTEREST

The authors declare that they have no conflicts of interest.

SUPPLEMENTARY INFORMATION

The online version contains supplementary material available at https://doi.org/10.1134/S1064229321100100.

The scheme of the formation of pedosediments.

REFERENCES

1. N. A. Agaev, Doctoral Dissertation in Agriculture (Moscow, 1990).
2. *Atlas of the USSR* (Main Directorate of Geodesy and Cartography under the Council of Ministers of the USSR, Moscow, 1947) [in Russian].
3. V. F. Babanin, V. I. Trukhin, L. O. Karpachevskii, A. V. Ivanov, and V. V. Morozov, *Soil Magnetism* (Yaroslavl State Technical University, Yaroslavl, 1995) [in Russian].
4. A. B. Bagdasaryan, *Climate of Armenian SSR* (Academy of Sciences of the Armenian SSR, Yerevan, 1958) [in Russian].
5. E. V. Belyaeva and V. P. Lyubin, "New data on the initial human settlement of the Southern Caucasus (Results of the fieldwork of the Armenian-Russian expedition in 2003 to 2018)," in *The Past of Humankind as seen by the Petersburg Archaeologists at the Dawn of the Millennium (to the Centennial of the Russian Academic Archaeology)* (Peterburgskoe Vostokovedenie, St. Petersburg, 2019) [in Russian]. https://doi.org/31.600/978-5-85803-525-1
6. E. V. Belyaeva, "Early Acheulian industries of the Transcaucasian upland and the adjacent areas of the Caucasus and the Near East," in *The Early Paleolithic Sites and Environments of the Caucasus and Adjacent Areas in the Early-Middle Pleistocene* (Peterburgskoe Vostokovedenie, St. Petersburg, 2020). https://doi.org/10.31600/978-5-85803-549-7-41-64
7. G. I. Bushinskii, "Titanium in sedimentogenesis process," Litol. Polezn. Iskop., No. 2, 73–82 (1963).
8. A. F. Vadyunina and Z. A. Korchagina, *Methods for Studying of Soil Physical Properties* (Agropromizdat, Moscow, 1986) [in Russian].
9. E. I. Gagarina, *Micromorphologic Analysis of Soils* (St. Petersburg State University, St. Petersburg, 2004) [in Russian].
10. *Geology of the USSR*, Vol. 43: *Armenian SSR*, Part 1: *Geological Description*, Ed. by A. T. Aslanyan, et al. (Nedra, Moscow, 1970) [in Russian].
11. R. G. Gracheva, I. V. Zamotaev, B. A. Il'ichev, and V. O. Targul'yan, *The Pattern of Structure of Soil Spatial Space of Tropics and Subtropics: Lithogenic Heritage, Self-Development, and Evolution. R&D Work No. 96-05-65511* (Moscow, 1996).
12. A. A. Golyeva, "An experience in using phytolithic analysis in soil science," Eurasian Soil Sci. **12**, 1498 (1995).
13. A. A. Gol'eva, *Phytolithes and Their Information Role in the Studies of Natural and Archeological Objects* (Moscow, 2001) [in Russian].
14. M. I. Dergacheva, *Archeological Soil Science* (Siberian Branch, Russian Academy of Sciences, Novosibirsk, 1997) [in Russian].
15. R. T. Dzhrbashyan, Kh. B. Meliksetyan, Yu. G. Gukasyan, R. P. Gevorgyan, I. Savov, S. G. Karapetyan, G. Kh. Navasardyan, and D. A. Manucharyan, "The Plinian eruption of Irind volcano (Aragats volcanic region, Armenia)," Izv. Nats. Akad. Nauk Resp. Arm., Nauki Zemle **68** (1), 3–21 (2015).
16. S. A. Inozemtsev and V. O. Targul'yan, *Upper Permian Paleosols: Properties, Processes, and Pedogenic Conditions* (GEOS, Moscow, 2010) [in Russian].
17. G. D. Isaev, "Classification of carbonate rocks and biosedimentology as the basis for regional facies analysis," Vestn. Tomsk. Gos. Univ., No. 332, 177–183 (2010).
18. N. A. Kachinskii, *Soil Physics* (Vysshaya Shkola, Moscow, 1965), Part 1.
19. V. A. Kovda, *Fundamental Theory on Soils. General Theory of Pedogenesis* (Nauka, Moscow, 1973) [in Russian].
20. V. A. Kovda and B. G. Rozanov, *Soil Science*, Part 1: *Soil and Pedogenesis* (Vysshaya Shkola, Moscow, 1988) [in Russian].
21. V. A. Kovda and B. G. Rozanov, *Soil Science*, Part 2 *Types, Geography, and Use of Soils* (Vysshaya Shkola, Moscow, 1988) [in Russian].
22. V. A. Kovda, I. V. Yakushevskaya, and A. N. Tyuryukanov, *Trace Elements in Soils of the Soviet Union* (Moscow, 1959) [in Russian]
23. A. M. Kuznetsova and O. S. Khokhlova, "Morphology of carbonate accumulations in soils of various types," Lithol. Miner. Resour. **45**, 89–100 (2010).
24. F. Yu. Levinson-Lessing, *Theoretical Petrography Related with Analysis of Erupted Rocks in Central Caucasus* (Tipogr. K. Matisena, Yurev, 1898) [in Russian].
25. S. N. Lesovaya, Doctoral Dissertation in Geography (St. Petersburg, 2006)

26. E. A. Lesnykh, "Behavior of trace elements in soil during the loss of humus by the example of soils of the Ob plateau of Altai krai," Vestn. Altaisk. Gos. Agrar. Univ., No. 3 (19), 27–30 (2005).
27. V. P. Lyubin, "Dzhraber Upper Acheulian industries (Armenia)," Kratk. Soobshch. Inst. Arkheol., Akad. Nauk SSSR, No. 82, 59–67 (1961).
28. V. P. Lyubin, E. V. Belyaeva, V. G. Trifonov, A. N. Simakova, D. V. Ozherel'ev, O. S. Khokhlova, A. A. Nosova, et al., "Dynamics of the environment and the formation of the ancient Early Paleolithic cultures of South-West Asia," in *Proceedings of the All-Russian Scientific Conf. "Natural Science Research Methods and the Paradigm of Modern Archeology," December 8–11, 2015* (Moscow, 2015), pp. 45–49.
29. A. K. Magak'yan, *Vegetation of Armenian SSR*, Kul'tiasov, M.V., Ed., (Academy of Sciences of USSR, Moscow, 1941) [in Russian].
30. Kh. B. Meliksetyan, "Geochemistry of volcanoes series in Aragatskaya oblast," Nats. Akad. auk Resp. Arm., Nauki Zemle, No. **3**, 34–59 (2012).
31. *National Atlas of Soils of Russian Federation*, Ed. by S. A. Shoba (Moscow, 2011) [in Russian].
32. N. G. Nurgalieva, *Reconstructive Role of Geochemical Data for the Study of Sedimentary Formations* (Kazan, 2017) [in Russian].
33. T. I. Rumyantseva, A. A. Lukshin, and V. P. Kovrigo, "Magnetic sensitivity of soils in general soil zones of the USSR," in *Soil Properties and Rational Use of Fertilizers*, Ed. by Yu. V. Shcherbakov (Perm, 1986), pp. 67–72.
34. S. N. Sedov, O. S. Khokhlova, and A. M. Kuznetsova, "Polygenesis of volcanic paleosols in Armenia and Mexico: Micromorphological records of climate variations in the quaternary period," Eurasian Soil Sci. **44**, 766–780 (2011).
35. I. A. Samofalova, O. B. Rogova, O. A. Luzyanina, and A. T. Savichev, "Geochemical features of the distribution of trace elements in soils of undisturbed landscapes of the middle Urals (by the example of the Basegi Nature Reserve)," Byull. Pochv. Inst. im. V.V. Dokuchaeva, No. 85, 56–76 (2016). https://doi.org/10.19047/0136-1694-2016-85-57-76
36. I. N. Spiridonova, *Specific Pedogenesis in the Late Bronze, Early Iron, and Early Middle Ages (Forest-Steppe of Central Volga Region)* (Penza, 2017) [in Russian].
37. E. M. Stolpnikova, Candidate's Dissertation in Biology (Moscow, 2017).
38. E. M. Stolpnikova and N. O. Kovaleva, "Characteristics of paleosols and pedosediments of the sites of primitive man in the valley of the Dzoraget River (Armenia)," Povozhsk. Ekol. Zh., No. 4, 628–642 (2014).
39. P. A. Sukhanov, A. D. Kashanskii, and V. D. Naumov, "Agrogenetic characteristics of rendzina soils of Tripolitania (Libya)," Izv. Timiryazevsk. S-kh. Akad., No. 1, 63–71 (2012).
40. *Tectonic Scheme of Armenian SSR, Scale 1 : 600000*, Ed. by A. T. Aslanyan and A. T. Veguni (Geological Institute, Academy of Sciences of USSR, Moscow, 1968) [in Russian].
41. S. N. Udal'tsov, T. V. Kuznetsova, and V. A. Demkin, "Carbon dioxide emission from modern and buried soils in dry steppes of the Lower Volga region," Vestn. Tomsk. Gos. Univ., Ser. Estestv. Tekh. Nauki **18** (3), 1014–1017 (2013).
42. O. S. Khokhlova and S. N. Sedov, "Pedogenic features in multilayer archaeological monuments of the Lower Pleistocene in northern Armenia and paleoclimatic reconstructions," in *Genesis, Diagnostics, and Prevention of Ecological Disasters* (MAKS Press, Moscow, 2017), pp. 90–112.
43. O. S. Khokhlova, T. N. Myakshina, A. N. Kuznetsov, and S. V. Gubin, "Morphogenetic features of soils in the Cat Tien National Park, southern Vietnam," Eurasian Soil Sci. **50**, 158–175 (2017). https://doi.org/10.1134/S1064229316120085
44. B. I. Chuvashov and A. L. Anfimov, "The origin of patterned limestones (by the example of Devonian and Permian carbonates of Ural)," Tr. Inst. Geol. Geokhim., Ural. Otd., Ross. Akad. Nauk, No. 156, 86–90 (2009).
45. L. V. Shtefan, *Fundamentals of Crystal Optics* (Belarusian State University, Minsk, 2002) [in Russian].
46. Ya. E. Yudovich and M. P. Ketris, *Fundamentals of Lithological Chemistry* (Nauka, St. Petersburg, 2000) [in Russian].
47. P. Fine, M. J. Singer, R. La Ven, K. Verosub, and R. J. Southard, "Role of pedogenesis in distribution of magnetic susceptibility in two California chronosequences," Geoderma **44**, 287–306 (1989).
48. S. Gallet, B. M. Jahn, and M. Torii, "Geochemical characterization of the Luochuan loess–paleosol sequence, China, and paleoclimatic implications," Chem. Geol. **133**, 67–88 (1996).
49. IUSS Working Group WRB, *World Reference Base for Soil Resources 2014, International Soil Classification System for Naming Soils and Creating Legends for Soil Maps, World Soil Resources Reports No. 106* (UN Food and Agriculture Organization, Rome, 2014).
50. O. S. Khokhlova, A. A. Khokhlov, A. M. Kuznetsova, E. M. Stolpnikova, N. O. Kovaleva, V. P. Lyubin, and E. V. Belyaeva, "Carbonate features in the uppermost layers of Quaternary deposits, Northern Armenia, and their significance for paleoenvironmental reconstruction," Quat. Int. **418**, 94–104 (2016). https://doi.org/10.1016/j.quaint.2015.07.035
51. O. S. Khokhlova, S. N. Sedov, A. A. Khokhlov, E. V. Belyaeva, and V. P. Lyubin, "Indications of pedogenesis in Lower Pleistocene tool-bearing sediments in Northern Armenia and regional paleoclimatic reconstruction," Quat. Int. **469**, 68–84 (2018). https://doi.org/10.1016/j.quaint.2016.10.040
52. J. P. Nguetnkam, E. Solleiro-Rebolledo, J. Díaz-Ortega, and P. Témati, "Evaluating weathering of palaeosols in Cameroon (Central Africa) as a tool for paleoenvironmental reconstruction," Catena **194**, 104688 (2020). https://doi.org/10.1016/j.catena.2020.104688
53. B. Ortega-Guerrero, S. Sedov, E. Solleiro-Rebolledo, and A. Soler, "Magnetic mineralogy in Barranca-Tlalpan exposure paleosols, Tlaxcala, Mexico," Rev. Mex. Cienc. Geol. **21** (1), 120–132 (2004).
54. D. R. Piperno, *Phytolith Analysis: An Archaeological and Geological Perspective* (Academic, San Diego, 1988).

55. S. L. Presnyakov, E. V. Belyaeva, V. P. Lyubin, N. V. Rodionov, A. V. Antonov, A. K. Saltykova, N. G. Berezhnaya, and S. A. Sergeev, "Age of the earliest Paleolithic sites in the northern part of the Armenian Highland by SHRIMP-II U–Pb geochronology of zircons from volcanic ashes," Gondwana Res. **21**, 929–938 (2012).

56. G. J. Retallack, "Soils and global change in the carbon cycle over geological time," in *Treatise on Geochemistry*, Vol. 5: *Surface and Ground Water, Weathering, and Soils* (Elsevier, Amsterdam, 2003), pp. 581–605.

57. G. J. Retallack, *Soils of the Past: an Introduction to Paleopedology* (Blackwell, Oxford, 2001).

58. N. E. Ryabogina, A. S. Afonin, S. N. Ivanov, H.-C. Li, P. A. Kalinin, S. N. Udaltsov, and S. A. Nikolaenko, "Holocene paleoenvironmental changes reflected in peat and lake sediment records of Western Siberia: geochemical and plant macrofossil proxies," Quat. Int. **528**, 73–87 (2019). https://doi.org/10.1016/j.quaint.2019.04.006

59. S. N. Sedov, O. S. Khokhlova, and A. M. Kuznetsova, "Polygenesis of volcanic paleosols in Armenia and Mexico: micromorphological records of climate variations in the Quaternary period," Eurasian Soil Sci. **44**, 766–780 (2011). https://doi.org/10.1134/S1064229311070118

60. V. G. Trifonov, V. P. Lyubin, E. V. Belyaeva, V. A. Lebedev, Ya. I. Trikhunkov, A. S. Tesakov, A. N. Simakova, et al., "Stratigraphic and tectonic settings of Early Paleolithic of North-West Armenia," Quart. Int. **420**, 178–198 (2016). https://doi.org/10.1016/j.quaint.2015.08.019

61. V. G. Trifonov, E. A. Shalaeva, L. Kh. Saakyan, D. M. Bachmanov, V. A. Lebedev, Ya. I. Trikhunkov, A. N. Simakova, A. V. Avagyan, et al., "Quaternary tectonics of recent basins in northwestern Armenia," Geotectonics **51** (5), 499–519 (2017).

Translated by I. Bel'chenko